Solid State Communications 151 (2011) 553–556

Contents lists available at ScienceDirect

Solid State Communications

journal homepage: www.elsevier.com/locate/ssc

Measurement of the absolute Raman cross section of the optical phonon in silicon

R.L. Aggarwal [a,*], L.W. Farrar [a], S.K. Saikin [b], A. Aspuru-Guzik [b], M. Stopa [c], D.L. Polla [d]

[a] MIT Lincoln Laboratory, Lexington, MA 02420-9108, USA
[b] Department of Chemistry and Chemical Biology, Harvard University, Cambridge, MA 02138, USA
[c] Department of Physics and Center for Nanoscale Systems, Harvard University, Cambridge, MA 02138, USA
[d] Defense Advanced Research Projects Agency, Arlington, VA 22203-1714, USA

ARTICLE INFO

Article history:
Received 24 December 2010
Accepted 16 January 2011
by A.H. MacDonald
Available online 25 January 2011

Keywords:
A. Semiconductors
B. Phonons
C. Inelastic light scattering

ABSTRACT

The absolute Raman cross section σ_{RS} of the first-order 519 cm^{-1} optical phonon in silicon was measured using a small temperature-controlled blackbody for the signal calibration of the Raman system. Measurements were made with a 25-mil thick (001) silicon sample located in the focal plane of a 20-mm effective focal length (EFL) lens using 785-, 1064-, and 1535-nm CW pump lasers for the excitation of Raman scattering. The pump beam was polarized along the [100] axis of the silicon sample. Values of $1.0\pm0.2\times10^{-27}$, $3.6\pm0.7\times10^{-28}$, and $1.1\pm0.2\times10^{-29}$ cm^2 were determined for σ_{RS} for 785-, 1064-, and 1535-nm excitation, respectively. The corresponding values of the Raman scattering efficiency S are $4.0\pm0.8\times10^{-6}$, $1.4\pm0.3\times10^{-6}$, and $4.4\pm0.8\times10^{-8}$ cm^{-1} sr^{-1}.The values of the Raman polarizability $|d|$ for 785-, 1064-, and 1535-nm excitation are $4.4\pm0.4\times10^{-15}$, $5.1\pm0.5\times10^{-15}$, and $1.9\pm0.2\times10^{-15}$ cm^2, respectively. The values of $4.4\pm0.4\times10^{-15}$ and $5.1\pm0.5\times10^{-15}$ cm^2 for $|d|$ for 785- and 1064-nm excitation, respectively, are 1.3 and 2.0 times larger than the values of 3.5×10^{-15} and 2.5×10^{-15} cm^2 calculated by Wendel. The Raman polarizability $|d|$ computed using the density functional theory in the long-wavelength limit is consistent with the general trend of the measured data and Wendel's model.

1. Introduction

Silicon is a semiconductor material that is most widely used for computer and other electronic devices. The crystal structure of silicon is that of diamond, which is face-centered cubic with a basis of two atoms at 000 and 1/4, 1/4, 1/4 associated with each lattice point [1]. There are eight atoms in a cubic unit cell and there are two atoms in the primitive unit cell, which contains lattice points at the corners only. Each atom has four nearest neighbors bonded in a tetrahedral arrangement. There are six phonon modes in silicon with two atoms in the primitive unit cell. Three of the phonon modes are triply-degenerate optical (LO + TO) modes, while two of the phonon modes are doubly-degenerate transverse acoustic (TA) modes, and finally, the remaining phonon mode is the longitudinal acoustic (LA) mode. The first-order Raman spectrum of the zone-center optical phonon of silicon was first observed by Russell in 1965 [2] using a 632.8-nm (1.96-eV) He–Ne laser as the excitation/pump source. Since then, the first-order Raman scattering of silicon has been studied by a number of groups. Parker et al. in 1967 [3] used an argon-ion laser operating at 488.0 nm (2.54 eV) to study the first-order Raman scattering of silicon and germanium. Hart et al. in 1970 [4] measured the temperature dependence of the frequency and linewidth of the zone-center optical phonon mode using an argon-ion laser operating at 514.5 nm (2.41 eV); part of this work is included in Kittel's textbook on *Introduction to Solid State Physics*, p. 445–446 [1]. The frequency of the $q = 0$ optical mode at room temperature has been determined to be $519\pm1cm^{-1}$ [4,5]. Ralston et al. in 1970 [6] measured the Raman cross section of the 519-cm^{-1} optical phonon mode relative to that of CS_2 using 1060-nm (1.17-eV), 1120-nm (1.11-eV), and 1320-nm (0.94-eV) pump lasers. The Raman cross section of the 519-cm^{-1} optical phonon mode of silicon has been computed by Wendel in 1979 [7] based on a pseudopotential calculation. An *ab initio* calculation of the Raman cross section of silicon was reported by Baroni and Resta in 1986 [8]. Measurement of the absolute Raman cross section of silicon was reported by Grimsditch and Cardona in 1980 [9] using the Brillouin scattering signal for the calibration of the Raman signal for pump lasers operating at 1.92 eV (646 nm), 2.41 eV (514.5 nm), 2.54 eV (488 nm), and 2.71 eV (457.6 nm). Wagner and Cardona in 1983 [10] have measured the Raman cross section of silicon using pump lasers at 1.16 eV (1069 nm) and 0.94 eV (1319 nm) by comparison with Raman scattering of diamond. We report on the measurement of the absolute Raman cross section of the 519-cm^{-1} optical phonon mode in room temperature silicon using a temperature-calibrated blackbody for the signal calibration of the Raman spectrometer [11] and pump lasers operating at 785 nm (1.58 eV), and 1535 nm (0.81 eV). The results for 1064-nm

* Corresponding author. Tel.: +1 781 981 0626; fax: +1 781 981 0602.
E-mail address: aggarwal@ll.mit.edu (R.L. Aggarwal).

0038-1098/$ – see front matter © 2011 Elsevier Ltd. All rights reserved.
doi:10.1016/j.ssc.2011.01.011

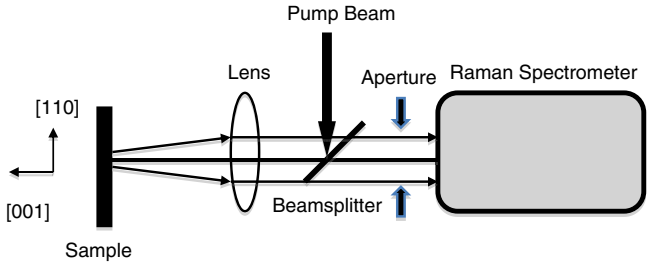

Fig. 1. Schematic of the optical setup for the measurement of Raman cross section; the sample is located in the focal plane of a 20-mm effective focal length (EFL) lens.

(1.17-eV) excitation were obtained with the silicon sample cooled to ∼80 K.

2. Experimental

The sample was cut from a 25-mil (0.63-mm) thick [001] silicon wafer polished on both sides. The edges of the sample were along the [110] and [1$\bar{1}$0] axes, which were oriented along the horizontal and vertical directions, respectively. This implies that the [100] and [010] axes of the sample were at ±45° to the vertical direction, which is parallel to the grooves of the gratings in the Raman spectrometers. The sample crystal orientation was confirmed with X-ray diffraction measurements. The sample was located in the focal plane of the focusing lens.

A schematic of the optical setup is shown in Fig. 1, which includes a Raman spectrometer, and a 45° beamsplitter for directing the pump beam onto the sample through the focusing lens that collects as well as collimates the Raman scattered light for its spectral analysis. The diameter of the focused pump beam was ∼40 μm.

The lens is a 12-mm diameter, 20-mm effective focal length (EFL) near-infrared (NIR) achromat Edmund Optics [12] part number 45–792. The 785-, 1064, and 1535-nm beamsplitters are dichroic and were procured from Chroma Technology [13]. The fraction of the scattered light collected is limited by a 7-mm diameter aperture, which is placed between the beamsplitter and the lens. The 785-nm pump laser is a 1400-mW CW single-mode, linearly polarized Sacher Lasertechnik [14] diode laser model SYS-420-0785-1400. The 1064-nm pump laser is a 10-W CW IPG Photonics [15] linearly polarized fiber laser model YLR-10-1064-LP. The 1535-nm pump is also a 10-W CW IPG Photonics [15] linearly polarized fiber laser model YLR-10-1535-LP.

The 785-, 1064-, and 1535-nm Raman spectrometers are DeltaNu [16] model Advantage 785, 1064, and 1535, respectively. The Advantage 785 is equipped with a silicon CCD camera MOSIR 350 [17]. The Advantage 1064 and 1535 are equipped with InGaAs cameras MOSIR 950 [17]. The grating in the Advantage 785 has 1800 grooves/mm. The gratings in the Advantage 1064 and Advantage 1535 have 830 grooves/mm. Each of the three Raman spectrometers includes two long-wave pass (LWP) filters and a 2x beam expander, which consists of two lenses of 20- and 40-mm EFL. A small pinhole is placed at the common focus of the beam expander to reduce unwanted radiation entering the camera in the Raman spectrometer. The diameter of the pinholes in the 785-, 1064- and 1535-nm Raman spectrometers is 100, 100, and 75 μm, respectively.

The Raman spectrometers were calibrated using a 50–1000 °C, small-cavity, unpolarized blackbody Electro Optical Industries [18] model CS 1000-008 with 85-mil (2.16-mm) aperture. The 85-mil aperture of the blackbody was covered with a 50-μm pinhole, which is comparable in size to that of the focused pump beam. The temperature of the blackbody was set at 675, 500, and 300 °C for the calibration of the 785-, 1064-, and 1535-nm Raman spectrometers, respectively.

3. Theoretical

The polarization unit vector $\boldsymbol{E_R}$ of the scattered light is related to that of the pump light $\boldsymbol{E_P}$ as

$$E_R = \frac{1}{d}\chi E_P, \tag{1}$$

where d is the Raman polarizability, and χ is the 3 × 3 Raman polarizability tensor. The Raman polarizability tensors for silicon referred to the cubic crystal axes x, y, and z, represented by [100], [010], and [001], respectively, are given by Loudon [19]

$$\chi_1 = \begin{bmatrix} 0 & 0 & 0 \\ 0 & 0 & d \\ 0 & d & 0 \end{bmatrix} \tag{2}$$

$$\chi_2 = \begin{bmatrix} 0 & 0 & d \\ 0 & 0 & 0 \\ d & 0 & 0 \end{bmatrix} \tag{3}$$

$$\chi_3 = \begin{bmatrix} 0 & d & 0 \\ d & 0 & 0 \\ 0 & 0 & 0 \end{bmatrix}. \tag{4}$$

In this experiment, the pump and scattered beams propagate along the z-axis. Therefore, the z-components of $\boldsymbol{E_P}$ and $\boldsymbol{E_R}$ must be zero. Furthermore, $\boldsymbol{E_P}$ is parallel to the x-axis. This implies that only χ_3 contributes to the scattering and that $\boldsymbol{E_R}$ is parallel to the y-axis, which is at 45° to the grooves of the gratings in the Raman spectrometers. Therefore, the grating diffraction efficiency for the scattered light is the same as that for the unpolarized blackbody radiation used for the calibration of the Raman spectrometers. The Raman collection efficiency is given by

$$\eta_c = \frac{D_A^2}{16n^2(\mathrm{EFL})^2}, \tag{5}$$

where D_A is the diameter of the aperture placed between the beamsplitter and the focusing lens and n is the refractive index of the sample at the wavelength of the scattered light. The value of D_A is 7 mm. The Raman cross section is given by

$$\sigma_{RS} = \frac{Fh\nu_p}{\eta_c P_p NL}, \tag{6}$$

where F is the integrated area under the Raman mode, $h\nu_P$ is the pump photon energy, P_P is the pump power incident upon the sample, N is the atomic concentration of silicon, and L is the effective thickness that contributes to scattering [9]. The value of N is 4.992 × 10^{22} atoms/cm^3, obtained using a value of 2.329 g/cm^3 [20] for the density of silicon at room temperature. Several authors use a Raman scattering efficiency S per unit length per unit solid angle, which is related to σ_{RS} as follows:

$$S = \frac{\sigma_{RS}N}{4\pi}. \tag{7}$$

The magnitude of the Raman polarizability $|d|$ is related to σ_{RS} as

$$|d| = \left(\frac{\rho c^4 \nu_R \sigma_{RS}}{8\pi^3 h \nu_S^4 N(n_0+1)}\right)^{\frac{1}{2}}, \tag{8}$$

where ρ is the mass density, ν_R is the Raman frequency (Hz) of the optical phonon mode, h is the Planck constant, ν_S is the frequency (Hz) of the Stokes component of the Raman scattered light, and n_0 is the optical phonon occupation number given by

$$n_0 = \frac{1}{e^{h\nu_R/kT} - 1}, \tag{9}$$

where T is the temperature.

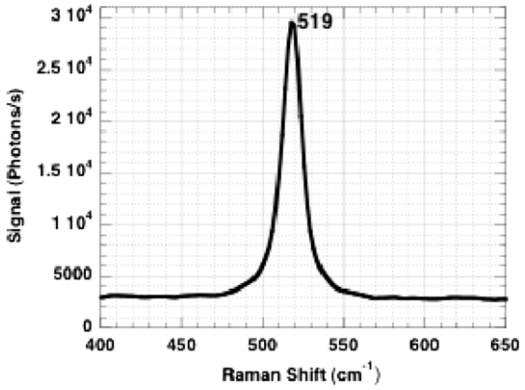

Fig. 2. Raman spectrum of 0.63-mm thick [001] silicon obtained with 9.2 mW of 785-nm excitation and 1.0-s integration time.

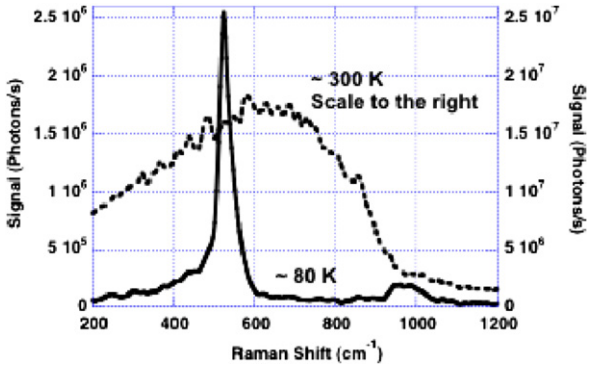

Fig. 3. Photoluminescence spectrum at ∼300 K (dotted curve) and Raman spectrum at ∼80 K (solid curve) of 0.63-mm thick [001] silicon obtained with 13.8 mW of 1064-nm excitation and 1.0-s integration time.

To estimate the value of d, Raman polarizability of the optical phonon modes was computed in the static limit within the density functional theory (DFT) in the local density approximation using the Quantum ESPRESSO package [21]. In the calculations the valence-core electron interaction was treated with a norm-conserving pseudo-potential [22]. The wavefunction was expanded in a plane-wave basis set with the 60 Ry cutoff. The irreducible part of the Brillouin zone was sampled with 2480 wave vectors spaced on a uniform grid. With the equilibrium lattice constant $a = 5.43$ Å and the atomic mass $m = 28.0855$ amu the frequency of the optical phonon modes computed at the Γ-point is 501 cm^{-1}. The corresponding value of the static Raman polarizability is $|d| = 3.0 \times 10^{-15}$ cm^2.

4. Results and discussion

785-nm *excitation*.

Fig. 2 shows the first-order Raman spectrum of the 519-cm^{-1} optical phonon mode of room-temperature Si obtained with 9.2 mW of 785-nm pump power on the sample and 1.0-s integration time.

The sample thickness L is given by

$$L = \frac{(1-R)^2}{2\alpha}, \tag{10}$$

where R is the reflectance of Si at the pump wavelength, and α is the average absorption coefficient for the pump and Raman wavelengths given by

$$\alpha = \frac{4\pi k}{\lambda}, \tag{11}$$

where k is the imaginary part of the refractive index. Using a value of 0.33 for R obtained using a value of 3.69 for n, 0.0065 for k [23], and 800 nm for λ, we obtain a value of 2.2 μm for L.

Using a value of 7 mm for D_A, 3.69 for n, and 20 mm for EFL, Eq. (5) yields a value of 5.59×10^{-4} for η_c. The value of F for the optical phonon in the spectrum of Fig. 2 is determined to be 2.27×10^5 using 489–549 cm^{-1} integration. Using this value of F, 2.53×10^{-19} J for $h\nu_P$, 5.6×10^{-4} for η_c, 9.2 mW for P_P, and 2.2 μm for L, Eq. (6) yields a value of $1.0 \pm 0.2 \times 10^{-27}$ cm^2 for σ_{RS}. Using this value of σ_{RS} and Eqs. (7)–(8), we obtain values of $4.0 \pm 0.8 \times 10^{-6}$ cm^{-1} sr^{-1} and $4.4 \pm 0.4 \times 10^{-15}$cm^2 for S and $|d|$, respectively. Our measured value of $4.4 \pm 0.4 \times 10^{-15}$ cm^2 for $|d|$ is 1.3 times larger than the calculated value of 3.5×10^{-15} cm^2, as obtained from the solid curve of Fig. 1 of Ref. [7] for 785-nm (1.58-eV) excitation.

The same optical setup was used to measure the Raman cross section of the 403-cm^{-1} LO phonon mode of a 1-mm thick GaP sample. We obtained a value of $2.7 \pm 0.5 \times 10^{-28}$ cm^2 for σ_{RS}, which is in excellent agreement with the value of $3.0 \pm 0.6 \times 10^{-28}$ cm^2 reported previously [9]. The value of $1.0 \pm 1.0 \times 10^{-27}$ cm^2 for σ_{RS} for the 519-cm^{-1} mode of Si is 3.3 times larger than that of $3.0 \pm 0.6 \times 10^{-28}$ cm^2 for the 403-cm^{-1} mode of GaP.

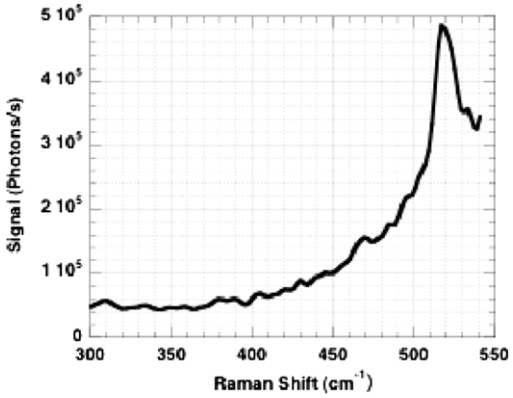

Fig. 4. Raman spectrum of 0.63-mm thick [001] silicon obtained with 11.5 mW of 1535-nm excitation and 1.0-s integration time.

1064-nm *excitation*.

We are unable to observe the Raman spectrum of silicon at room temperature (∼300 K) for the 1064-nm excitation because of relatively strong photoluminescence, as shown in Fig. 3. However, upon cooling the sample to liquid nitrogen temperature (∼80 K), photoluminescence disappears and the first-order Raman spectrum of the optical phonon mode of silicon is observed at 524-cm^{-1}, as shown in Fig. 3.

The observed optical phonon frequency (524 cm^{-1}) at 80 K is in agreement with the data of Ref. [4]. The value of F for the optical phonon in Fig. 3 is determined to be 4.34×10^7 using an integration between 450–600 cm^{-1}. Using this value of F, 1.865×10^{-19} J for $h\nu_P$, 6.25×10^{-4} for η_c, 13.8 mW for P_P, and 0.52 mm for L, Eq. (6) yields a value of $3.6 \pm 0.7 \times 10^{-28}$ cm^2 for σ_{RS}. Subsequently, employing the value of σ_{RS} and Eqs. (7)–(8), we obtain values of $1.4 \pm 0.3 \times 10^{-6}$ cm^{-1} sr^{-1} and $5.1 \pm 0.5 \times 10^{-15}$ cm^2 for S and $|d|$, respectively. Our measured value of $|d|$ is 2 times larger than the calculated value of 2.5×10^{-15} cm^2 in Ref. [7]; this may be due to a relatively weak resonance enhancement arising from the indirect band gap.

1535-nm *excitation*.

Fig. 4 shows the first-order Raman spectrum of the 519-cm^{-1} optical phonon mode of room-temperature Si obtained with 11.5 mW of 1535-nm pump power on the sample and 1.0-s integration time.

Table 1
Summary of the measured and computed values of σ_{RS}, S and $|d|$.

$h\nu_P$ (eV)	σ_{RS} (cm^2)	S (cm^{-1} sr^{-1})	$\|d\|$ (cm^2)
0 (Static limit)	–	–	3.0×10^{-15}
0.81 (This work)	$1.1\pm0.2\times10^{-29}$	$4.4\pm0.9\times10^{-8}$	$1.9 \pm 0.2 \times 10^{-15}$
0.94 (Ref. [10])	$3.1\pm1.1\times10^{-29}$	$1.2\pm0.4\times10^{-7}$	$2.3 \pm 0.4 \times 10^{-15}$
1.16 (Ref. [10])	$8.0\pm2.8\times10^{-29}$	$3.2\pm1.1\times10^{-7}$	$2.3 \pm 0.4 \times 10^{-15}$
1.17 (This work)	$3.6\pm0.7\times10^{-28}$	$1.4\pm0.3\times10^{-6}$	$5.1 \pm 0.5 \times 10^{-15}$
1.58 (This work)	$1.0\pm0.2\times10^{-27}$	$4.0\pm0.8\times10^{-6}$	$4.4 \pm 0.4 \times 10^{-15}$
1.92 (Ref. [9])	$7.9\pm5.5\times10^{-27}$	$3.1\pm2.2\times10^{-5}$	$8.0 \pm 2.8 \times 10^{-15}$
2.41 (Ref. [9])	$5.2\pm2.3\times10^{-26}$	$2.1\pm0.9\times10^{-4}$	$1.28 \pm 0.28 \times 10^{-14}$
2.54 (Ref. [9])	$5.6\pm2.6\times10^{-26}$	$2.2\pm0.9\times10^{-4}$	$1.21 \pm 0.28 \times 10^{-14}$
2.71 (Ref. [9])	$7.1\pm3.3\times10^{-26}$	$2.8\pm1.3\times10^{-4}$	$1.18 \pm 0.28 \times 10^{-14}$

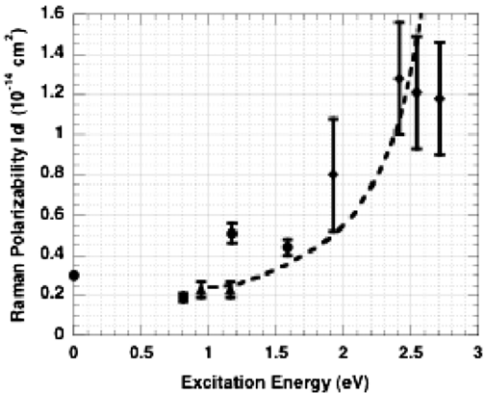

Fig. 5. Plot of the Raman polarizability $|d|$ of silicon versus excitation energy. The data point at 0 eV represents the value calculated from first principles in the static limit. Circles, triangles, and diamonds represent data points from this work, and Refs. [10,9], respectively. The dashed curve represents values calculated by Wendel [7].

The value of F for the optical phonon in Fig. 4 is determined to be 1.69×10^6 using 493–541 cm^{-1} integration. Using this value of F, 1.293×10^{-19} J for $h\nu_P$, 5.6×10^{-4} for η_c, 11.5 mW for P_P, and 0.52 mm for L, Eq. (6) yields a value of $1.1 \pm 0.2 \times 10^{-29}$ cm^2 for σ_{RS}. With this value of σ_{RS} and Eqs. (7)–(8), we obtain values of $4.4 \pm 0.9 \times 10^{-8}$ cm^{-1} sr^{-1} and $1.9 \pm 0.2 \times 10^{-15}$ cm^2 for S and $|d|$, respectively. Our measured value of $1.9 \pm 0.2 \times 10^{-15}$ cm^2 for $|d|$ using 1535-nm (0.81-eV) excitation cannot be compared with the calculated value of $|d|$, because results are not available for excitation wavelengths longer than 1240 nm for which the value of $|d|$ is 2.3×10^{-15} cm^2.

Our measured values of σ_{RS}, S, and $|d|$ as well as some others are given in Table 1. The values of $|d|$ given in Refs. [9,10] were used to obtain the values of σ_{RS} and S given in Table 1. The data point at 0 eV in Table 1 represents the value calculated from first principles in the static limit.

A plot of the Raman polarizability $|d|$ versus excitation energy is shown in Fig. 5. The data is in good agreement with Wendel's calculated values, shown as the dashed curve in Fig. 5. The computed static value of the Raman polarizability is consistent with the long wavelength limit extrapolation of the measured data.

5. Conclusions

Our values of the absolute Raman scattering cross sections of silicon in terms of $|d|$ for 785- and 1064-nm excitation, obtained using a temperature-controlled blackbody for the signal calibration of the Raman spectrometers, are in good agreement (within a factor of 2) with the values calculated by Wendel [7]. The static limit extrapolation of the Raman polarizability also agrees with the value computed using Quantum ESPRESSO DFT code.

Acknowledgements

We thank Dan Calawa for X-ray orientation of the silicon sample and Dr. T.Y. Fan for his comments on this paper. The work at MIT Lincoln Laboratory was sponsored by the Defense Advanced Research Projects Agency under Air Force Contract FA8721-05-C-0002. The work at Harvard University was sponsored by the Defense Advanced Research Projects Agency under Air Force Contract FA9550-08-1-0285 and by the Defense Threat Reduction Agency under Contract No. HDTRA1-10-1-0046. Opinions, interpretation, and recommendations are those of the authors, and do not necessarily represent the view of the United States Government.

References

[1] See, for example C. Kittel, Introduction to Solid State Physics, eighth ed., John Wiley & Sons, New York, 2005, p. 16.
[2] J.P. Russell, Appl. Phys. Lett. 11 (1965) 223.
[3] J.H. Parker Jr., D.W. Feldman, M. Ashkin, Phys. Rev. 155 (1967) 712.
[4] T.R. Hart, R.L. Aggarwal, B. Lax, Phys. Rev. B 1 (1970) 638.
[5] P.A. Temple, C.E. Hathway, Phys. Rev. B 7 (1973) 3685.
[6] J.M. Ralston, R.L. Wadsack, R.K. Chang, Phys. Rev. Lett. 25 (1970) 814.
[7] H. Wendel, Solid State Commun. 31 (1979) 423.
[8] S. Baroni, R. Resta, Phys. Rev. B 33 (1986) 5969.
[9] M. Grimsditch, M. Cardona, Phys. Status Solidi B 102 (1980) 155.
[10] J. Wagner, M. Cardona, Solid State Commun. 48 (1983) 301.
[11] R.L. Aggarwal, L.W. Farrar, D.L. Polla, Solid State Commun. 149 (2009) 1330.
[12] Edmund optics, Barrington, NJ 08007-1380, USA.
[13] Chroma Technology Corp., Rockingham, VT 05101, USA.
[14] Sacher Lasertechnik, Marburg, Germany, Buena Park, CA 90620, USA.
[15] IPG Photonics, Oxford, MA 01540, USA.
[16] DeltaNu, Laramie, WY 82020, USA.
[17] Intevac, Inc., Santa Clara, CA 95054, USA.
[18] Electro optical industries, Santa Barbara, CA 93111, USA.
[19] R. Loudon, Adv. Phys. 13 (1964) 423.
[20] H.A. Bowman, R.M. Schoonover, C.L. Carroll, J. Res. Natl. Bur. Stand. A 78 (1974) 13.
[21] P. Giannozzi, et al., J. Phys.: Condens. Matter 21 (2009) 395502.
[22] We used the Si.pz-vbc. UPF pseudopotential from: http://www.quantum-espresso.org.
[23] E.D. Palik (Ed.), Handbook of Optical Constants of Solids, Academic Press, 1985, p. 565.